



Fermi National Accelerator Laboratory

FERMILAB-Pub-98/334-E

CDF

**Events with a Rapidity Gap Between Jets
in $\bar{p}p$ Collisions at $\sqrt{s} = 630$ GeV**

F. Abe et al.

The CDF Collaboration

*Fermi National Accelerator Laboratory
P.O. Box 500, Batavia, Illinois 60510*

November 1998

Submitted to *Physical Review Letters*

Disclaimer

This report was prepared as an account of work sponsored by an agency of the United States Government. Neither the United States Government nor any agency thereof, nor any of their employees, makes any warranty, expressed or implied, or assumes any legal liability or responsibility for the accuracy, completeness, or usefulness of any information, apparatus, product, or process disclosed, or represents that its use would not infringe privately owned rights. Reference herein to any specific commercial product, process, or service by trade name, trademark, manufacturer, or otherwise, does not necessarily constitute or imply its endorsement, recommendation, or favoring by the United States Government or any agency thereof. The views and opinions of authors expressed herein do not necessarily state or reflect those of the United States Government or any agency thereof.

Distribution

Approved for public release; further dissemination unlimited.

Copyright Notification

This manuscript has been authored by Universities Research Association, Inc. under contract No. DE-AC02-76CHO3000 with the U.S. Department of Energy. The United States Government and the publisher, by accepting the article for publication, acknowledges that the United States Government retains a nonexclusive, paid-up, irrevocable, worldwide license to publish or reproduce the published form of this manuscript, or allow others to do so, for United States Government Purposes.

Events with a rapidity gap between jets in $\bar{p}p$ collisions at $\sqrt{s} = 630$ GeV

F. Abe,¹⁷ H. Akimoto,³⁹ A. Akopian,³¹ M. G. Albrow,⁷ A. Amadon,⁵ S. R. Amendolia,²⁷ D. Amidei,²⁰ J. Antos,³³
 S. Aota,³⁷ G. Apollinari,³¹ T. Arisawa,³⁹ T. Asakawa,³⁷ W. Ashmanskas,¹⁸ M. Atac,⁷ P. Azzi-Bacchetta,²⁵
 N. Bacchetta,²⁵ S. Bagdasarov,³¹ M. W. Bailey,²² P. de Barbaro,³⁰ A. Barbaro-Galtieri,¹⁸ V. E. Barnes,²⁹
 B. A. Barnett,¹⁵ M. Barone,⁹ G. Bauer,¹⁹ T. Baumann,¹¹ F. Bedeschi,²⁷ S. Behrends,³ S. Belforte,²⁷ G. Bellettini,²⁷
 J. Bellinger,⁴⁰ D. Benjamin,³⁵ J. Bensinger,³ A. Beretvas,⁷ J. P. Berge,⁷ J. Berryhill,⁵ S. Bertolucci,⁹ S. Bettelli,²⁷
 B. Bevensee,²⁶ A. Bhatti,³¹ K. Biery,⁷ C. Bigongiari,²⁷ M. Binkley,⁷ D. Bisello,²⁵ R. E. Blair,¹ C. Blocker,³ S. Blusk,³⁰
 A. Bodek,³⁰ W. Bokhari,²⁶ G. Bolla,²⁹ Y. Bonushkin,⁴ D. Bortoletto,²⁹ J. Boudreau,²⁸ L. Breccia,² C. Bromberg,²¹
 N. Bruner,²² R. Brunetti,² E. Buckley-Geer,⁷ H. S. Budd,³⁰ K. Burkett,²⁰ G. Busetto,²⁵ A. Byon-Wagner,⁷
 K. L. Byrum,¹ M. Campbell,²⁰ A. Caner,²⁷ W. Carithers,¹⁸ D. Carlsmith,⁴⁰ J. Cassada,³⁰ A. Castro,²⁵ D. Cauz,³⁶
 A. Cerri,²⁷ P. S. Chang,³³ P. T. Chang,³³ H. Y. Chao,³³ J. Chapman,²⁰ M. -T. Cheng,³³ M. Chertok,³⁴ G. Chiarelli,²⁷
 C. N. Chiou,³³ F. Chlebana,⁷ L. Christofek,¹³ M. L. Chu,³³ S. Cihangir,⁷ A. G. Clark,¹⁰ M. Cobal,²⁷ E. Cocca,²⁷
 M. Contreras,⁵ M. E. Convery,³¹ J. Conway,³² J. Cooper,⁷ M. Cordelli,⁹ D. Costanzo,²⁷ C. Couyoumtzelis,¹⁰
 D. Cronin-Hennessy,⁶ R. Culbertson,⁵ D. Dagenhart,³⁸ T. Daniels,¹⁹ F. DeJongh,⁷ S. Dell'Agnello,⁹ M. Dell'Orso,²⁷
 R. Demina,⁷ L. Demortier,³¹ M. Deninno,² P. F. Derwent,⁷ T. Devlin,³² J. R. Dittmann,⁶ S. Donati,²⁷ J. Done,³⁴
 T. Dorigo,²⁵ N. Eddy,²⁰ K. Einsweiler,¹⁸ J. E. Elias,⁷ R. Ely,¹⁸ E. Engels, Jr.,²⁸ W. Erdmann,⁷ D. Errede,¹³
 S. Errede,¹³ Q. Fan,³⁰ R. G. Feild,⁴¹ Z. Feng,¹⁵ C. Ferretti,²⁷ I. Fiori,² B. Flaughner,⁷ G. W. Foster,⁷ M. Franklin,¹¹
 J. Freeman,⁷ J. Friedman,¹⁹ H. Frisch,⁵ Y. Fukui,¹⁷ S. Gadomski,¹⁴ S. Galeotti,²⁷ M. Gallinaro,²⁶ O. Ganel,³⁵
 M. Garcia-Sciveres,¹⁸ A. F. Garfinkel,²⁹ C. Gay,⁴¹ S. Geer,⁷ D. W. Gerdes,¹⁵ P. Giannetti,²⁷ N. Giokaris,³¹ G. Giusti,²⁷
 M. Gold,²² A. Gordon,¹¹ A. T. Goshaw,⁶ Y. Gotra,²⁸ K. Goulianos,³¹ H. Grassmann,³⁶ L. Groer,³² C. Grosso-Pilcher,⁵
 G. Guillian,²⁰ J. Guimaraes da Costa,¹⁵ R. S. Guo,³³ C. Haber,¹⁸ E. Hafen,¹⁹ S. R. Hahn,⁷ R. Hamilton,¹¹ T. Handa,¹²
 R. Handler,⁴⁰ F. Happacher,⁹ K. Hara,³⁷ A. D. Hardman,²⁹ R. M. Harris,⁷ F. Hartmann,¹⁶ J. Hauser,⁴ E. Hayashi,³⁷
 J. Heinrich,²⁶ W. Hao,³⁵ B. Hinrichsen,¹⁴ K. D. Hoffman,²⁹ M. Hohmann,⁵ C. Holck,²⁶ R. Hollebeek,²⁶ L. Holloway,¹³
 Z. Huang,²⁰ B. T. Huffman,²⁸ R. Hughes,²³ J. Huston,²¹ J. Huth,¹¹ H. Ikeda,³⁷ M. Incagli,²⁷ J. Incandela,⁷
 G. Introzzi,²⁷ J. Iwai,³⁹ Y. Iwata,¹² E. James,²⁰ H. Jensen,⁷ U. Joshi,⁷ E. Kajfasz,²⁵ H. Kambara,¹⁰ T. Kamon,³⁴
 T. Kaneko,³⁷ K. Karr,³⁸ H. Kasha,⁴¹ Y. Kato,²⁴ T. A. Keaffaber,²⁹ K. Kelley,¹⁹ R. D. Kennedy,⁷ R. Kephart,⁷
 D. Kestenbaum,¹¹ D. Khazins,⁶ T. Kikuchi,³⁷ B. J. Kim,²⁷ H. S. Kim,¹⁴ S. H. Kim,³⁷ Y. K. Kim,¹⁸ L. Kirsch,³
 S. Klimenko,⁸ D. Knoblauch,¹⁶ P. Koehn,²³ A. Königter,¹⁶ K. Kondo,³⁷ J. Konigsberg,⁸ K. Kordas,¹⁴ A. Korytov,⁸
 E. Kovacs,¹ W. Kowald,⁶ J. Kroll,²⁶ M. Kruse,³⁰ S. E. Kuhlmann,¹ E. Kuns,³² K. Kurino,¹² T. Kuwabara,³⁷
 A. T. Laasanen,²⁹ S. Lami,²⁷ S. Lammel,⁷ J. I. Lamoureux,³ M. Lancaster,¹⁸ M. Lanzoni,²⁷ G. Latino,²⁷ T. LeCompte,¹
 S. Leone,²⁷ J. D. Lewis,⁷ M. Lindgren,⁴ T. M. Liss,¹³ J. B. Liu,³⁰ Y. C. Liu,³³ N. Lockyer,²⁶ O. Long,²⁶ C. Loomis,³²
 M. Loreti,²⁵ D. Lucchesi,²⁷ P. Lukens,⁷ S. Lusin,⁴⁰ J. Lys,¹⁸ K. Maeshima,⁷ P. Maksimovic,¹¹ M. Mangano,²⁷
 M. Mariotti,²⁵ J. P. Marriner,⁷ G. Martignon,²⁵ A. Martin,⁴¹ J. A. J. Matthews,²² P. Mazzanti,² K. McFarland,³⁰
 P. McIntyre,³⁴ P. Melese,³¹ M. Menguzzato,²⁵ A. Menzione,²⁷ E. Meschi,²⁷ C. Mesropian,³¹ S. Metzler,²⁶ C. Miao,²⁰
 T. Miao,⁷ G. Michail,¹¹ R. Miller,²¹ H. Minato,³⁷ S. Miscetti,⁹ M. Mishina,¹⁷ S. Miyashita,³⁷ N. Moggi,²⁷ E. Moore,²²
 Y. Morita,¹⁷ A. Mukherjee,⁷ T. Muller,¹⁶ P. Murat,²⁷ S. Murgia,²¹ M. Musy,³⁶ H. Nakada,³⁷ T. Nakaya,⁵ I. Nakano,¹²
 C. Nelson,⁷ D. Neuberger,¹⁶ C. Newman-Holmes,⁷ C.-Y. P. Ngan,¹⁹ L. Nodulman,¹ A. Nomerotski,⁸ S. H. Oh,⁶
 T. Ohmoto,¹² T. Ohsugi,¹² R. Oishi,³⁷ M. Okabe,³⁷ T. Okusawa,²⁴ J. Olsen,⁴⁰ C. Pagliarone,²⁷ R. Paoletti,²⁷
 V. Papadimitriou,³⁵ S. P. Pappas,⁴¹ N. Parashar,²⁷ A. Parri,⁹ J. Patrick,⁷ G. Pauletta,³⁶ M. Paulini,¹⁸ A. Perazzo,²⁷
 L. Pescara,²⁵ M. D. Peters,¹⁸ T. J. Phillips,⁶ G. Piacentino,²⁷ M. Pillai,³⁰ K. T. Pitts,⁷ R. Plunkett,⁷ A. Pompos,²⁹
 L. Pondrom,⁴⁰ J. Proudfoot,¹ F. Ptohos,¹¹ G. Punzi,²⁷ K. Ragan,¹⁴ D. Reher,¹⁸ M. Reischl,¹⁶ A. Ribon,²⁵ F. Rimondi,²
 L. Ristori,²⁷ W. J. Robertson,⁶ T. Rodrigo,²⁷ S. Rolli,³⁸ L. Rosenson,¹⁹ R. Roser,¹³ T. Saab,¹⁴ W. K. Sakumoto,³⁰
 D. Saltzberg,⁴ A. Sansoni,⁹ L. Santi,³⁶ H. Sato,³⁷ P. Schlabach,⁷ E. E. Schmidt,⁷ M. P. Schmidt,⁴¹ A. Scott,⁴
 A. Scribano,²⁷ S. Segler,⁷ S. Seidel,²² Y. Seiya,³⁷ F. Semeria,² T. Shah,¹⁹ M. D. Shapiro,¹⁸ N. M. Shaw,²⁹
 P. F. Shepard,²⁸ T. Shibayama,³⁷ M. Shimojima,³⁷ M. Shochet,⁵ J. Siegrist,¹⁸ A. Sill,³⁵ P. Sinervo,¹⁴ P. Singh,¹³
 K. Sliwa,³⁸ C. Smith,¹⁵ F. D. Snider,¹⁵ J. Spalding,⁷ T. Speer,¹⁰ P. Sphicas,¹⁹ F. Spinella,²⁷ M. Spiropulu,¹¹
 L. Spiegel,⁷ L. Stanco,²⁵ J. Steele,⁴⁰ A. Stefanini,²⁷ R. Ströhmer,^{7a} J. Strologas,¹³ F. Strumia,¹⁰ D. Stuart,⁷
 K. Sumorok,¹⁹ J. Suzuki,³⁷ T. Suzuki,³⁷ T. Takahashi,²⁴ T. Takano,²⁴ R. Takashima,¹² K. Takikawa,³⁷ M. Tanaka,³⁷
 B. Tannenbaum,²² F. Tartarelli,²⁷ W. Taylor,¹⁴ M. Tecchio,²⁰ P. K. Teng,³³ Y. Teramoto,²⁴ K. Terashi,³⁷ S. Tether,¹⁹
 D. Theriot,⁷ T. L. Thomas,²² R. Thurman-Keup,¹ M. Timko,³⁸ P. Tipton,³⁰ A. Titov,³¹ S. Tkaczyk,⁷ D. Toback,⁵
 K. Tollefson,³⁰ A. Tollestrup,⁷ H. Toyoda,²⁴ W. Trischuk,¹⁴ J. F. de Troconiz,¹¹ S. Truitt,²⁰ J. Tseng,¹⁹ N. Turini,²⁷
 T. Uchida,³⁷ F. Ukegawa,²⁶ J. Valls,³² S. C. van den Brink,²⁸ S. Vejcek, III,²⁰ G. Velev,²⁷ R. Vidal,⁷ R. Vilar,^{7a}
 D. Vucinic,¹⁹ R. G. Wagner,¹ R. L. Wagner,⁷ J. Wahl,⁵ N. B. Wallace,²⁷ A. M. Walsh,³² C. Wang,⁶ C. H. Wang,³³
 M. J. Wang,³³ A. Warburton,¹⁴ T. Watanabe,³⁷ T. Watts,³² R. Webb,³⁴ C. Wei,⁶ H. Wenzel,¹⁶ W. C. Wester, III,⁷
 A. B. Wicklund,¹ E. Wicklund,⁷ R. Wilkinson,²⁶ H. H. Williams,²⁶ P. Wilson,⁵ B. L. Winer,²³ D. Winn,²⁰

D. Wolinski,²⁰ J. Wolinski,²¹ S. Worm,²² X. Wu,¹⁰ J. Wyss,²⁷ A. Yagil,⁷ W. Yao,¹⁸ K. Yasuoka,³⁷ G. P. Yeh,⁷
P. Yeh,³³ J. Yoh,⁷ C. Yosef,²¹ T. Yoshida,²⁴ I. Yu,⁷ A. Zanetti,³⁶ F. Zetti,²⁷ and S. Zucchelli²

(CDF Collaboration)

- ¹ Argonne National Laboratory, Argonne, Illinois 60439
² Istituto Nazionale di Fisica Nucleare, University of Bologna, I-40127 Bologna, Italy
³ Brandeis University, Waltham, Massachusetts 02254
⁴ University of California at Los Angeles, Los Angeles, California 90024
⁵ University of Chicago, Chicago, Illinois 60637
⁶ Duke University, Durham, North Carolina 27708
⁷ Fermi National Accelerator Laboratory, Batavia, Illinois 60510
⁸ University of Florida, Gainesville, Florida 32611
⁹ Laboratori Nazionali di Frascati, Istituto Nazionale di Fisica Nucleare, I-00044 Frascati, Italy
¹⁰ University of Geneva, CH-1211 Geneva 4, Switzerland
¹¹ Harvard University, Cambridge, Massachusetts 02138
¹² Hiroshima University, Higashi-Hiroshima 724, Japan
¹³ University of Illinois, Urbana, Illinois 61801
¹⁴ Institute of Particle Physics, McGill University, Montreal H3A 2T8, and University of Toronto,
Toronto M5S 1A7, Canada
¹⁵ The Johns Hopkins University, Baltimore, Maryland 21218
¹⁶ Institut für Experimentelle Kernphysik, Universität Karlsruhe, 76128 Karlsruhe, Germany
¹⁷ National Laboratory for High Energy Physics (KEK), Tsukuba, Ibaraki 305, Japan
¹⁸ Ernest Orlando Lawrence Berkeley National Laboratory, Berkeley, California 94720
¹⁹ Massachusetts Institute of Technology, Cambridge, Massachusetts 02139
²⁰ University of Michigan, Ann Arbor, Michigan 48109
²¹ Michigan State University, East Lansing, Michigan 48824
²² University of New Mexico, Albuquerque, New Mexico 87131
²³ The Ohio State University, Columbus, Ohio 43210
²⁴ Osaka City University, Osaka 588, Japan
²⁵ Università di Padova, Istituto Nazionale di Fisica Nucleare, Sezione di Padova, I-35131 Padova, Italy
²⁶ University of Pennsylvania, Philadelphia, Pennsylvania 19104
²⁷ Istituto Nazionale di Fisica Nucleare, University and Scuola Normale Superiore of Pisa, I-56100 Pisa, Italy
²⁸ University of Pittsburgh, Pittsburgh, Pennsylvania 15260
²⁹ Purdue University, West Lafayette, Indiana 47907
³⁰ University of Rochester, Rochester, New York 14627
³¹ Rockefeller University, New York, New York 10021
³² Rutgers University, Piscataway, New Jersey 08855
³³ Academia Sinica, Taipei, Taiwan 11530, Republic of China
³⁴ Texas A&M University, College Station, Texas 77843
³⁵ Texas Tech University, Lubbock, Texas 79409
³⁶ Istituto Nazionale di Fisica Nucleare, University of Trieste/ Udine, Italy
³⁷ University of Tsukuba, Tsukuba, Ibaraki 315, Japan
³⁸ Tufts University, Medford, Massachusetts 02155
³⁹ Waseda University, Tokyo 169, Japan
⁴⁰ University of Wisconsin, Madison, Wisconsin 53706
⁴¹ Yale University, New Haven, Connecticut 06520

We report a measurement of the fraction of dijet events with a rapidity gap between jets produced by color-singlet exchange in $\bar{p}p$ collisions at $\sqrt{s} = 630$ GeV at the Fermilab Tevatron. In events with two jets of transverse energy $E_T^{jet} > 8$ GeV, pseudorapidity in the range $1.8 < |\eta^{jet}| < 3.5$ and $\eta_1 \eta_2 < 0$, the color-singlet exchange fraction is found to be $R = [2.7 \pm 0.7(\text{stat}) \pm 0.6(\text{syst})]\%$. Comparisons are made with results obtained at $\sqrt{s} = 1800$ GeV and with theoretical expectations.

PACS number(s): 13.87.Fh, 12.38.Qk, 13.85.Hd

Experiments in $\bar{p}p$ collisions at $\sqrt{s}=1800$ GeV at the Fermilab Tevatron [1–3] and in photoproduction at $135 < W_{\gamma p} < 280$ GeV at HERA [4] have established the existence and measured the rate of production of events with a rapidity gap between jets attributed to a strongly interacting color-singlet exchange (CSE). A rapidity gap is a region in pseudorapidity [5] in which there are no charged or neutral particles. In the usual production of jets through the exchange of a quark or a gluon, particles associated with the net color flow are commonly present between the jets. Rapidity gaps may be formed by fluctuations in the particle multiplicity, but the probability for such gaps is expected to decrease exponentially with increasing gap width. In contrast, a CSE signal should not depend strongly on gap size. This feature has been proposed [6] as a signature for CSE production. The fraction of CSE to all dijet events was measured to be $\sim 1\%$ at the Tevatron and $\sim 7\%$ at HERA. No strong dependence of this fraction was found [3] on jet transverse energy, E_T^{jet} , or pseudorapidity separation between the jets, $\Delta\eta$.

Models proposed [6–16] to describe the Tevatron and HERA data may be distinguished by their predictions for the CSE fraction and its dependence on E_T^{jet} , $\Delta\eta$ and \sqrt{s} . In this paper, we present a measurement of the CSE fraction and its E_T^{jet} and $\Delta\eta$ dependence for dijet events at $\sqrt{s} = 630$ GeV, and compare the results with those we obtained at $\sqrt{s} = 1800$ GeV [3] and with theoretical expectations.

This study is modeled after our study at 1800 GeV [3], in which the CSE signal in events with two jets of $E_T^{jet} > 20$ GeV, $1.8 < |\eta^{jet}| < 3.5$ and $\eta_1\eta_2 < 0$ was extracted from an analysis of the particle multiplicity distribution in the (central) pseudorapidity region $|\eta| < 1$. The scaling variables x_T and x of these jets, corresponding to the transverse and longitudinal momentum fractions of the interacting partons, are given by $x_T = 2E_T/\sqrt{s}$ and $x \approx (x_T/2)e^{|\eta|}$. The events collected at 630 GeV contain jets within the same η -region as the events at 1800 GeV, but with $E_T^{jet} > 8$ GeV, so that the same η^{jet} at the two energies corresponds approximately to the same x -value. At both energies, the E_T^{jet} was defined as the sum of the calorimeter E_T within an $\eta - \phi$ cone of 0.7 (see [17] for jet clustering algorithm). The components of the CDF detector relevant to this study have been described in [3].

The 630 GeV data sample consists of 2760 events with two or more jets above the jet E_T cut of 8 GeV. Events are classified as same-side (SS) if $\eta_1\eta_2 > 0$ and opposite-side (OS) if $\eta_1\eta_2 < 0$. There are 1420 SS and 1340 OS events in the data sample, of which 934 SS and 860 OS have one reconstructed vertex within $|z_{vtx}| < 60$ cm and are used in this analysis. Events with no reconstructed vertex ($< 1\%$) are included in this “single-vertex” sample. The single-vertex requirement was imposed to reject events due to multiple $\bar{p}p$ interactions producing one or more additional “minimum bias” (MB) events. An overlay of one or more MB events on a dijet event could

obscure a rapidity gap. At the average luminosity of $\langle \mathcal{L} \rangle = 1.3 \times 10^{30} \text{ cm}^{-2} \text{ s}^{-1}$ of the 630 GeV run, 17.6% of all dijet events are expected to have additional interactions.

As in the 1800 GeV study [3], we search for the CSE rapidity gap signal in the OS sample by comparing OS particle multiplicity distributions within a fixed central η -region between the jets with corresponding distributions of the SS sample, for which no central rapidity gaps due to CSE are expected [3]. For the purpose of this analysis, a “particle” is defined as a track of $p_T > 300$ MeV/c or a calorimeter tower of *detector* $E_T > 200$ MeV, corresponding to a *true* $E_T > \sim 300$ MeV.

Figure 1 shows (a) the track and (b) the calorimeter tower multiplicity distributions in the regions $|\eta| < 0.9$ for OS events and $|\eta| < 1.05$ ($|\eta| < 1.2$) for tracks (towers) for SS events. The widths of the SS η -regions were chosen larger than those of the OS η -regions to ensure the same mean values of track and tower multiplicity. The SS distributions were normalized to the number of OS events in the regions with $N_{track} > 0$ or $N_{tower} > 2$; the normalization factor was $C = 0.89$. Also shown in Fig. 1 are distributions for the difference between OS and SS multiplicities, normalized to the SS, defined as $D \equiv (N_{OS} - N_{SS})/N_{SS}$, where N_{OS} (N_{SS}) is the number of OS (SS) events in each bin. As an uncertainty in D we take $\delta D \equiv \sqrt{(1+C)/N_{SS}}$, which represents the 1σ deviation of the OS distribution from an expectation based on the SS distribution. A CSE signal should appear as an excess in D in the $N_{track} = 0$ bin; in the tower case, the excess is expected to spill over into the next two bins due to calorimeter noise and possibly γ 's from decays of π^0 's associated with the jets [3]. The mean values of the differences expected in the $N_{track} = 0$ bin, D_0^{trk} , and in the $N_{tower} = 0, 1, 2$ bins, $D_{0,1,2}^{tower}$, for normal color exchange (CE) are shown as open circles; they were evaluated by extrapolating fits (solid lines) made to the values of D in the regions of $N_{track} > 0$ and $N_{tower} > 2$. To account for possible small differences in the overall shapes of the OS and SS distributions, quadratic rather than linear fits were used. The excess seen in the $N_{track} = 0$ bin and in the (combined) $N_{tower} = 0, 1, 2$ bins is attributed to CSE. The CSE signal may be evaluated independently from the track or tower distribution using $N_{CSE} = N_{OS} - N_{CE}$, where N_{CE} is the expectation from CE. In the case of tracks, $N_{CE} = N_{SS} \cdot (1 + D_0^{trk} \pm \delta D_0^{trk})$; for towers, the first three bins are used.

The track distributions, Figs. 1(a,c), have 60 OS and $C \times 38 = 33.9$ (normalized) SS events in the $N_{track} = 0$ bin, where the extrapolated difference is $D_0^{trk} = -0.11 \pm 0.13$. These numbers yield $N_{CE} = [33.9 \pm 5.5(stat)] \cdot (1 + D_0^{trk} \pm \delta D_0^{trk}) = 30.2 \pm 6.6$ and $N_{CSE} = 29.8 \pm 7.7(stat) \pm 6.6(syst)$, where as statistical uncertainty in N_{CSE} we take the $\sqrt{N_{OS}} = \sqrt{60} = 7.7$ and as systematic the uncertainty in N_{CE} . The expected number of $N_{CE} = 30.2 \pm 6.6$ events could fluctuate with a standard deviation $\sigma = \sqrt{6.6^2 + 30.2} = 8.6$. Based

on an expectation of 30.2 ± 8.6 OS events from CE, the probability of a statistical fluctuation to ≥ 60 events is 2.3×10^{-4} (3.5σ).

In the case of tower multiplicities there are 70 OS and $C \times 45 = 40$ SS events in the first three bins. Following the same procedure, we find $N_{CSE} = 29.1 \pm 8.4$ (*stat*) ± 7.9 (*syst*), which is consistent with the result obtained from tracking. Because of the correlation expected between track and tower multiplicities, both for CSE and CE events, we will use below only the tracking result to evaluate the CSE fraction.

The single-vertex selection cut, which was imposed to reject events from multiple interactions, also rejects single interaction events with extra vertices caused by confusion in reconstruction due to the high particle multiplicities. For CE events, the single-vertex efficiency is $[79 \pm 3$ (*syst*)]%, determined by the ratio of the measured fraction of single-vertex events (65.0%) to the fraction expected from the instantaneous luminosity (82.4%). For CSE events, the efficiency is found to be 100^{+0}_{-3} % by comparing the number of rapidity gap events in the single-vertex sample with the number in the entire sample. Using the number of CSE events from the track multiplicity analysis and correcting it for the single-vertex efficiency, the fraction of CSE to all dijet events is found to be

$$R_{630} = [2.7 \pm 0.7(\text{stat}) \pm 0.6(\text{syst}) = 2.7 \pm 0.9]\%$$

At $\sqrt{s} = 1800$ GeV, the measured CSE fraction was [3] $R_{1800} = [1.13 \pm 0.12(\text{stat}) \pm 0.11(\text{syst}) = 1.13 \pm 0.16]\%$. The ratio of the CSE fractions at the two energies is

$$R_{630/1800} = 2.4 \pm 0.7(\text{stat}) \pm 0.6(\text{syst}) = 2.4 \pm 0.9$$

We have studied some properties of the CSE signal by comparing distributions obtained from the following three samples of events: (a) the ‘‘gap’’ sample, consisting of the events with both $N_{\text{track}} = 0$ and $N_{\text{tower}} = 0, 1, 2$ – these events contain the CSE signal, as well as a background due to CE, estimated from an analysis of the two-dimensional track-tower OS and SS distributions to be $(45 \pm 12)\%$; (b) a ‘‘control’’ sample, consisting of the events with 1-3 tracks and 0-6 hit towers; and (c) the ‘‘total’’ OS dijet sample. Comparisons are made between the ratios of gap/total and control/total events. Kinematic constraints imposed by the rapidity gap requirement, as well as systematic uncertainties due to detector effects, such as tracking efficiencies, largely cancel out in comparing these ratios, so that any differences seen may be reasonably attributed to the CSE content of the gap sample.

Figure 2 shows the ratios of number of gap and control sample events to the total number of OS events, corrected for the single-vertex efficiency, as a function of $\eta^* \equiv |\eta_1 - \eta_2|/2$, which is half the rapidity interval between the jets, and as a function of the average E_T of the two jets, E_T^* . The control sample distributions are normalized to the estimated 45% background in the gap sample. The CSE fractions, obtained by subtracting

the background from the gap distributions and normalizing to the tracking result, are compared with those from $\sqrt{s} = 1800$ GeV in Fig. 3.

We have also extracted the CSE fractions at the two energies as a function of the scaling variables x and x_T of the jets. The results are shown in Fig. 4 (a,b) as a function of (a) x_1, x_2 (two entries per event), and (b) x_T^* , the mean value of the x_T of the two leading jets. The solid (dashed) horizontal lines in Figs. 3,4 (a,b) represent the average value of the CSE fraction, R_{1800} (R_{630}). The $\chi^2/d.o.f.$ of the data points relative to the average fraction is 1.53 (0.98), 0.31 (0.66), 0.30 (0.31) and 0.31 (0.66) for the η^* , E_T^* , x and x_T^* distributions at 1800 (630) GeV, respectively.

In general, the CSE fraction shows no strong dependence on η^* , E_T^* , x or x_T^* . In the statistically more significant 1800 GeV data, the η^* distribution appears to drop at large η^* , while the E_T^* (x_T^*) distribution is consistent with being flat. The x -dependence is remarkably flat over the entire region of the measurement, $0.1 < x < 0.7$.

In Fig. 4 (c,d) the x and x_T distributions of the CSE fraction of the 1800 GeV data are compared with the corresponding distributions of the ratio of CE dijet events due to quark-(anti)quark scattering to all CE dijet events produced by a HERWIG [18] Monte Carlo simulation (solid line), including a simulation of the CDF detector. The rise of the ratio with x and x_T^* reflects the increase with x of the quark fraction of the (anti)proton parton distribution function. Adjusting the overall normalization of the Monte Carlo result to yield the best fit to the data, we obtained a $\chi^2/d.o.f.$ of 1.90 (0.48) for the x (x_T^*) distribution, respectively. While the x_T^* distribution of the data is compatible with both the HERWIG result and with being flat, the measured x distribution clearly favors a flat behavior. If the CSE coupled to quarks but not to gluons, the CSE fraction would be expected to follow the HERWIG result. The observed flat x -dependence indicates that the relative strength of the CSE effective coupling to quarks and gluons is comparable in magnitude to that of the CE coupling.

In the original two-gluon CSE model proposed by Bjorken [6], the CSE fraction is expected to depend weakly on η^* and decrease with increasing \sqrt{s} [7,8]. However, a more recent calculation, which unitarizes the gluon exchange amplitude [9] and uses a gap survival probability and a phase shift as free parameters, allows for CSE fractions which can increase or decrease with increasing η^* . Calculations [10] using a model [11] based on the BFKL formalism [12] of resummation of a color-singlet gluon ladder exchange predict a ‘‘basically flat’’ [13] η^* -distribution for the CSE fraction. In ‘‘soft color’’ models [14,15] gaps are formed in normal CE interactions by (non-perturbative) color rearrangements by soft quarks and gluons. A model applied to the Tevatron [15], in which the CSE signal is dominated by quark-(anti)quark scattering, predicts CSE fractions that rise with x and x_T^* in a manner similar to that of the HERWIG Monte Carlo curves shown in Fig. 4 (c,d).

The same behavior is predicted by a model based on a hypothetical light U(1) gauge boson, which couples only to baryon number, proposed [16] to account for the observed rate of rapidity gap production.

In conclusion, we find that a fraction $R = [2.7 \pm 0.7(stat) \pm 0.6(syst)]\%$ of events with two jets of $E_T > 8$ GeV, $|\eta| > 1.8$ and $\eta_1\eta_2 < 0$ produced in $\bar{p}p$ collisions at $\sqrt{s} = 630$ GeV have a rapidity gap attributed to color-singlet exchange. The ratio of R measured at 630 GeV to that at 1800 GeV is $2.4 \pm 0.7(stat) \pm 0.6(syst)$. The distribution of the CSE fraction as a function of dijet x_T^* is compatible with being flat, although not inconsistent with the rising behavior expected for an exchange that couples only to (anti)quarks. The shape of the distribution in jet η separation is also approximately flat, dropping somewhat at large $\Delta\eta$. The CSE fraction does not appear to depend on jet x over the range $0.1 < x < 0.7$ of our measurement. The x -dependence of the CSE/CE fraction probes the effective coupling of the CSE to quarks and gluons relative to the coupling of a single gluon. If the CSE coupled predominantly to quarks (gluons), the CSE fraction would be expected to increase (decrease) with increasing x . Within the limits imposed by the uncertainties in the data points, the observed flat x dependence suggests that the CSE and CE couplings to quarks and gluons have the same relative strength.

We thank the Fermilab staff and the technical staffs of the participating institutions for their vital contributions. This work was supported by the U.S. Department of Energy and National Science Foundation; the Italian Istituto Nazionale di Fisica Nucleare; the Ministry of Education, Science and Culture of Japan; the Natural Sciences and Engineering Research Council of Canada; the National Science Council of the Republic of China; and the A. P. Sloan Foundation.

-
- [1] F. Abe *et al.*, (CDF Collaboration), Phys. Rev. Lett. **74**, 855 (1995).
[2] S. Abachi *et al.* (DØ Collaboration), Phys. Rev. Lett. **76**, 734 (1996).
[3] F. Abe *et al.*, (CDF Collaboration), Phys. Rev. Lett. **80**, 1156 (1998).
[4] M. Derrick *et al.* (ZEUS Collaboration), Phys. Lett. B **369**, 55 (1996).
[5] The pseudorapidity, η , is defined as $\eta = -\ln \tan \frac{\theta}{2}$, where θ is the polar angle from the beam axis. We use the terms rapidity and pseudorapidity interchangeably.
[6] J. D. Bjorken, Phys. Rev. **D47**, 101 (1993).
[7] H. Chehime *et al.*, Phys. Lett. B **286**, 397 (1992).
[8] E. Gotsman, E. M. Levin and U. Maor, Phys. Lett. **B309**, 199 (1993); *ib.* hep-ph/9804404.
[9] R. Oeckl and D. Zeppenfeld, Phys. Rev. **D58**, 14003 (1998).

- [10] V. Del Duca and W.-K. Tang, Phys. Lett. **B312**, 225 (1993).
[11] A.H.Mueller and W.-K.Tang, Phys. Lett. **B284**, 123 (1992).
[12] L. N. Lipatov, Sov. J. Nucl. Phys. **23**, 338 (1976); E. A. Kuraev, L. N. Lipatov and V. S. Fadin, Sov. Phys. JETP **44**, 443 (1976); Sov. Phys. JETP **45**, 199 (1977); Ya. Ya. Balitskii and L. N. Lipatov, Sov. J. Nucl. Phys. **28**, 822 (1978).
[13] V. Del Duca, Proceedings of the 10th Topical Workshop on Proton-Antiproton Collider Physics, Fermilab, 9-13 May 1995, p. 648.
[14] A. Edin, G. Ingelman and J. Rathsman, Z. Phys. **C75**, 57 (1997).
[15] O. J. P. Eboli, E. M. Gregores and F. Halzen, MAD/PH-97-995 (1997), hep-ph/9708283.
[16] C. D. Carone and H. Murayama, Phys. Rev. Lett. **74**, 3122 (1995); C. D. Carone and H. Murayama, Phys. Rev. **D52**, 484 (1995).
[17] F. Abe *et al.*, (CDF Collaboration), Phys. Rev. **D45**, 1448 (1992).
[18] G. Marchesini, B.R. Webber, G. Abbiendi, I.G. Knowles, M.H. Seymour and L. Stanco, Comput. Phys. Comm. **67**, 465 (1992).

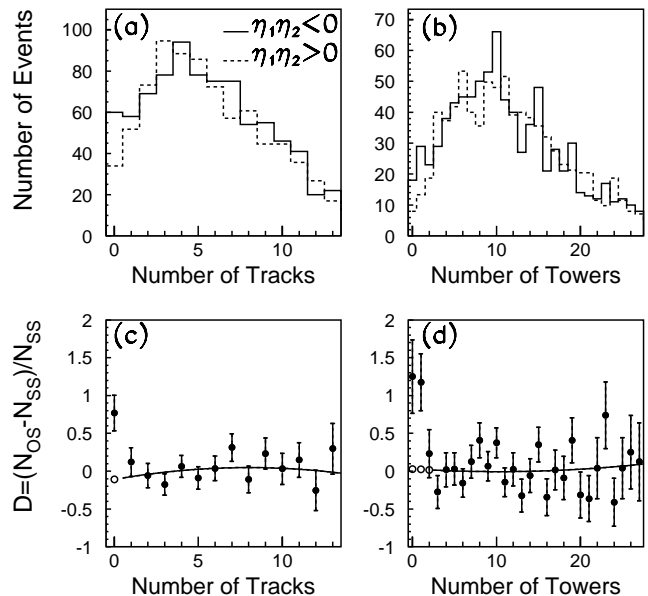


FIG. 1. (*top*) Multiplicity distributions (a) for tracks and (b) for calorimeter towers in the regions $|\eta| < 0.9$ for opposite-side (OS, $\eta_1\eta_2 < 0$) dijet events (solid lines), and $|\eta| < 1.05$ ($|\eta| < 1.2$) for tracks (towers) for same-side (SS, $\eta_1\eta_2 > 0$) dijet events (dashed lines); (*bottom*) the bin-by-bin difference between OS and SS events normalized to the number of SS events. The SS distribution is scaled to the OS by the ratio of OS/SS events for $N_{track} > 0$ in (a) and for $N_{tower} > 2$ in (b).

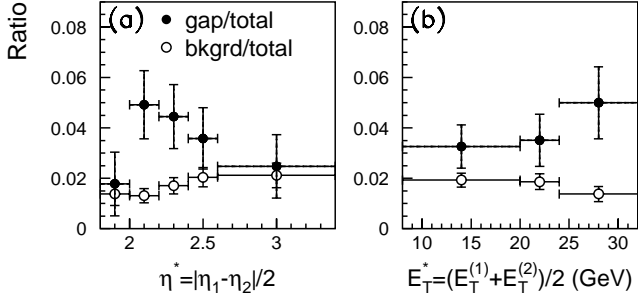


FIG. 2. Ratios at 630 GeV of gap events (solid points) and background events (open circles: control sample events normalized to the estimated 45% background) to all events as a function of (a) half the pseudorapidity separation between the jets and (b) the average transverse energy of the jets.

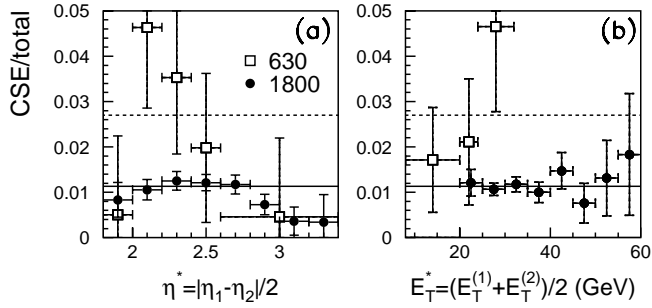


FIG. 3. Ratio of color-singlet exchange to total number of events at 630 and 1800 GeV as a function of (a) half the pseudorapidity separation between the jets and (b) the average transverse energy of the jets. The solid (dashed) lines represent the average ratio R_{1800} (R_{630}).

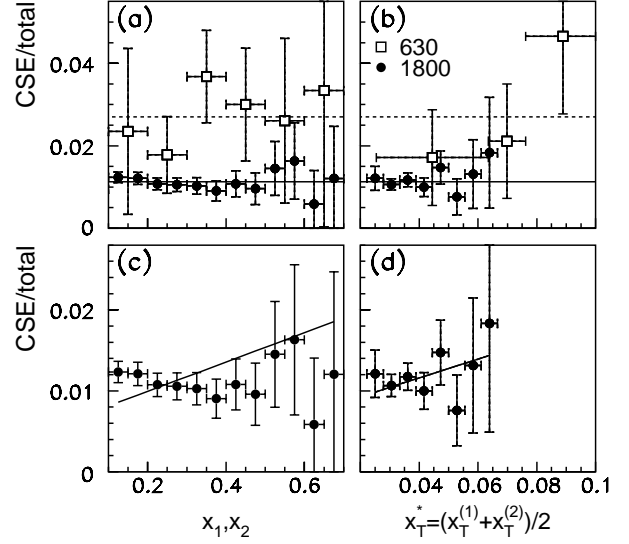


FIG. 4. Ratio of color-singlet exchange to total number of events at 630 (open squares) and 1800 (black circles) GeV as a function of (a,c) x , the ratio of the jet momentum along the beam to the momentum of the beam (two entries per event, one for each of the two leading jets) and (b,d) x_T^* , the average scaled transverse energy of the two jets. The solid (dashed) lines in (a,b) represent the average ratio R_{1800} (R_{630}). The solid lines in (c,d) represent the distributions of the fraction of CE dijet events due to quark-(anti)quark scattering to all CE dijet events produced by a HERWIG Monte Carlo simulation, including a simulation of the CDF detector. The normalization of the Monte Carlo result was adjusted to yield the best fit to the data.